Catal Lett (2008) 126:134–141
DOI 10.1007/s10562-008-9594-2

Influence of Citric Acid on Size Distribution of Ru Particles and the Catalytic Activities of the Ru/AC Catalysts

Jun Ni · Rong Wang · Jianxin Lin · Kemei Wei

Received: 5 June 2008 / Accepted: 15 July 2008 / Published online: 13 August 2008

Abstract Citric acid (CA) was used to modify graphited activated carbon (AC) for improving size distribution of Ru particles and catalytic activity of the Ru/AC catalyst. The influence of CA on the texture of AC and Ru/AC, Ru distribution and catalytic activity were investigated. TEM, TGA, TPD-MS, CO pulse chemisorption and N_2 physisorption indicate that CA modified AC creates more functional groups and thus more homogeneous dispersion of Ru nanoparticles. TEM images show most of the Ru particles were ca. 2–2.5 nm for the CA4 + Ru4/AC catalyst. The increase of ammonia synthesis activity for Ru–Ba–K/AC catalyst is more than 16% when the content of CA in AC is 4 wt.% at 673 K and 10,000 h^{-1}.

Keywords Citric acid · Ruthenium · Dispersion · Activity · Ammonia synthesis

1 Introduction

Ruthenium catalysts have been used in various catalytic reactions, such as the hydrogenolysis of glycerol [1–3], isomerization of linoleic acid [4], selective hydrogenation of benzene, Fischer–Tropsch synthesis [5–7] and ammonia synthesis [8–15]. But the high cost of precious metal hinders a broad application. The difference of the performance price ratio on various precursors was very notable, and the low-cost precursors have high performance price ratio. The main precursors for ruthenium catalysts are $Ru_3(CO)_{12}$, $RuCl_3$, $Ru(acac)_2$, $RuNO(NO_3)_3$, etc. Generally, $Ru_3(CO)_{12}$ or other chlorine-free ruthenium compounds rather than the stable and cheap $RuCl_3$ are employed as ruthenium precursor since the presence of chlorine usually significantly decreases the catalytic activity for ammonia synthesis. At present, the relatively cheaper precursor of $RuCl_3$ is gradually adopted in ruthenium catalysts because of high performance price ratio and improvement of dechlorination method. However, the ruthenium dispersion in Ru/AC catalyst with $RuCl_3$ as precursor is low, and particle size is non-uniform, which is not favorable to the full use of ruthenium [16–19].

One of the focuses for ruthenium-based catalyst is how to increase the activated sites of ruthenium and improve the utilization ratio of ruthenium [17, 18, 20–22]. Previous studies involved ruthenium dispersion on carbon are mainly concerned with the pre-treatment of $RuCl_3$ and support. Some researchers have investigated pre-reduction of $RuCl_3$ and modification of support in order to increase the effective utilization ratio of ruthenium. Recently, a sol–gel process of $RuCl_3$ for preparing well-defined Ru nanoparticles was focused [23–25]. However, the process still had some inevitable problems involving use of non-aqueous solvent, recovery of ruthenium and time-consuming preparation procedures. The problems are the main obstacles of its extensive application.

When graphite or graphitized materials are used as supports, they often require a pretreatment under oxidizing conditions to generate surface functionalities as anchoring sites for ionic species to be adsorbed from solution and finally to fix the metal crystallites. The dispersion of the supported metallic phase may be low at industrially interesting metal loadings for the support without such a pretreatment. The oxidation of carbon support with HNO_3, H_2O_2 or O_3 has been found to introduce functional groups

J. Ni · R. Wang · J. Lin · K. Wei (✉)
National Research Center of Chemical Fertilizer Catalysts, Fuzhou University, 523 Gongye Road, Fuzhou, Fujian 350002, People's Republic of China
e-mail: weikemei@163.com

on the surface of carbon nanotubes and thereby provide nucleation sites for the deposition of highly dispersed metal particles [26–30]. The surface oxidation methods, however, are often time-consuming process with high preparative cost. These methods are not favorable to wide adoption in supported catalysts. Carbon materials can be easily functionalized using citric acid (CA) without the disadvantage mentioned above. It has been reported that CA was used to modify a commercially activated carbon (AC) to improve copper ion adsorption from aqueous solutions [31]. Poh et al. [32] demonstrated that CA modified AC creates more functional groups and thus deposits more Pt nanoparticles with smaller average particle size on the surface of carbon materials for fuel cell applications. Citric acid can be used to modify AC for improving adsorption of heavy metal ions and pore structure of AC [31–34]. However, CA is seldom used to improve the size distribution of Ru particles and increase the unit amount of B_5 active sites.

Here we report an unique approach to connect protected Ru nanoparticles to graphitized AC by means of CA, rather than oxidant. Firstly, CA provides nucleation sites for the deposition of highly dispersed $RuCl_3$ before reduction. Then the anchorage is provided by CA residues capping the Ru and AC after reduction of catalysts. Since the structure and chemistry of AC treated with CA are dissimilar before and after reduction, functionalization of AC through CA will restrain the conglomeration of precious metals on the surface of AC and increase the dispersion of metals. The preparation method is simple, rapid and suitable for large-scale preparation. The ruthenium nanoparticles in the Ru/AC catalyst treated with CA were uniform and high dispersed. Furthermore, the activities of ammonia synthesis for the Ru/AC catalysts treated with proper level of CA are significantly higher than of the Ru/AC catalyst. These results indicate that CA modification is a promising technique of ruthenium catalyst preparation.

2 Experimental

2.1 Materials

$RuCl_3\ nH_2O$ (n = 1–3. 37 wt.% of Ru content), citric acid (denoted CA), $Ba(NO_3)_2$ and KOH are used as starting materials. All chemicals used in these experiments were analytical reagent grade and used without further treatment. The graphited activated carbon (denoted AC) was sieved into 12–16 mesh.

2.2 Sample Preparations

The graphited AC was impregnated with CA and $RuCl_3$ in aqueous solution at room temperature. The content of CA in AC were 2, 4, 8, and 12 wt.%, respectively, and the nominal Ru loading was 4.0 wt% in AC. The solvent was evaporated after impregnation by drying in infrared light. The samples was reduced in a stream of $3H_2 + N_2$ gas mixture at 723 K for 8 h, cooled to room temperature in the same flowing gas mixture, and slowly passivated by exposure to ambient air. The samples are referred to as CA2 + Ru4/AC, CA4 + Ru4/AC, CA8 + Ru4/AC, and CA12 + Ru4/AC, respectively.

The promoters were introduced by impregnating with an aqueous solution of $Ba(NO_3)_2$ and followed KOH, and then the sample was evaporated and dried by drying in infrared light. The contents of Ba and K promoters were 4 and 12 wt.%, respectively.

2.3 Characterization of Carbon Supports and Ruthenium Catalysts

The morphologies and particle size of Ru were studied by using transmission electron microscopy (TEM, Tecnai G2 F20 S-TWIN). N_2 adsorption–desorption was performed on an ASAP-2020H (Micromeritics Corp) instrument. The pore volume was calculated from the adsorbed volume at a relative pressure of 0.99. The specific surface area, the pore size distribution and the micropore volume were calculated by BET, BJH and t-plot method, respectively. The chemisorption study was carried out by using an AutoChem 2910 instrument (Micromeritics). Prior to the measurements, the catalyst (ca. 250 mg) was reduced in a H_2 stream at 723 K for 1.5 h, and then flushed with a helium stream for 1.5 h to remove H_2 adsorbed on the surface of the catalyst, and it was finally cooled in a helium stream to 323 K. CO chemisorption was measured by the pulse method by introducing CO flowing over the sample maintained at 298 K. Ru dispersion was calculated from the cumulative volume of CO adsorbed during pulse, assuming a chemisorption stoichiometry CO/Ru = 1:1. He-TPD-MS study was carried out using the apparatus described above for CO chemisorption experiments. The experiment was performed by heating sample at a rate of 10 C/min from room temperature to 1123 K under a He flow (30 mL/min). The effluents (m/e = 28 for CO, 44 for CO_2) were monitored by an online mass spectrometer (Pfeiffer vacuum, OmniStar).

2.4 Activity Studies

The ammonia synthesis was measured in a stainless steel reactor. Before activity testing, the catalysts (2 mL) with particle size of 12–16 meshes were activated in a stoichiometric H_2 and N_2 mixture (473, 573, 673, 723 and 773 K for 2 h, respectively), and then stabilized under the reaction conditions (i.e., 10 MPa, 673 K, 10,000 h^{-1} and H_2/N_2 = 3:1) for more than 2 h. The ammonia concentration in

the effluent was determined by a chemical titration method [35].

3 Results and Discussion

3.1 Effect of Citric Acid on Texture of Activated Carbon

Figure 1 shows the effect of loading of CA on pore size of AC. Addition of CA has an obvious influence on the micropore volume, but the effect on mesopores is very little, which proves CA was adsorbed preferentially in micropore. The decrease of pore volume is contributed mainly by adsorption of CA in micropore. It is consistent with the conclusion about adsorption of CA in microporous of AC [31]. The micropore volume decreases with the increase of content of CA in AC, but the most probable pore size and the mesopores volume has not significant change between CA, CA4/AC, CA8/AC and CA12/AC. These show that the adsorption of CA in micropore increases with the increase of addition of CA in AC. The most probable pore size has not significant change since the saturated absorption of CA in AC is much higher than 12 wt.%. In the experiment, the saturated adsorption of CA in the AC is ca. 60 wt.%.

Table 1 shows the effect of content of CA on texture of AC. The addition of CA influences remarkably the texture of AC. From Table 1 it can be seen that the pore volume and specific surface area of AC decrease obviously with the increase of loading of CA, and the pore size increases with the increase of CA in support. The specific surface area and pore volume decrease rapidly over 10% even the loading of CA is only 2 wt.%. The specific surface area decrease ca. 25% and the pore size increases only ca. 3.6% when the loading of CA is 4 wt.%. The notable decline of specific surface area arises from microporous blockage by adsorbed

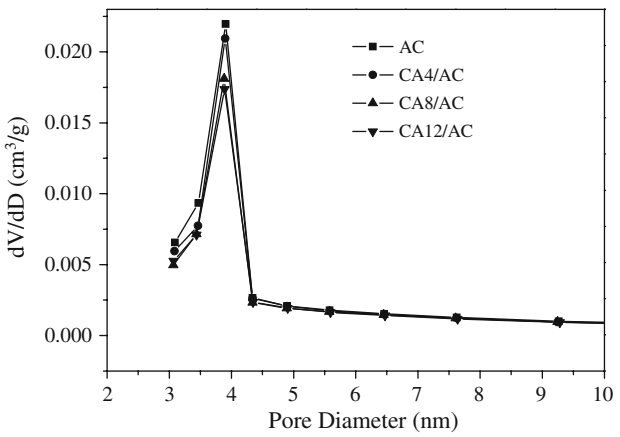

Fig. 1 Effect of loading of CA on pore size of AC

Table 1 Effect of loading of CA on texture of AC

Sample	Specific surface area (m^2/g)	Pore volume (cm^3/g)	Average pore size (nm)
AC	938	0.66	2.8
CA2/AC	782	0.57	2.9
CA4/AC	700	0.54	3.1
CA8/AC	577	0.48	3.3
CA12/AC	523	0.45	3.5

Table 2 Effect of loading of CA on texture of the Ru/AC catalysts

Sample	Specific surface area (m^2/g)	Pore volume (cm^3/g)	Pore size (nm)
AC	938	0.66	2.8
Ru/AC	847	0.61	2.9
CA2 + Ru4/AC	861	0.63	2.9
CA4 + Ru4/AC	863	0.62	2.9
CA8 + Ru4/AC	863	0.63	2.9
CA12 + Ru4/AC	855	0.61	2.8

CA molecules. Microporous blockage is favorable for the Ru/AC supported catalysts. Partial Ru particles must be located in small mesopores and micropores as ultra-fine, probably poorly organized nanoparticles [36]. These ultra-fine Ru nanoparticles (<1.5 nm) has few active sites for the activity [13]. Therefore, microporous blockage decreases the Ru content in micropores, which is favorable to the full use of ruthenium.

The effect of loading of CA on texture of the Ru/AC catalysts is shown in Table 2. The catalysts were reduced in a stream of $3H_2 + N_2$ gas mixture at 723 K for 8 h. Specific surface area of the catalysts treated with CA increases little for the Ru/AC catalyst. Addition of CA almost has little influence on average pore size of the Ru/AC catalysts, which is different from the results of Table 1. These results indicated that CA in catalyst almost had decomposed after pre-reduction of catalysts. The residual carbon has little influence on the specific surface area, pore volume and average pore size of Ru/AC catalyst.

3.2 Surface Functional Groups

Acidic oxidation treatment not only breaks carbon by eliminating the amorphous carbon, but also introduces a more hydrophilic surface structure and a larger number of oxygen-containing functional groups such as carboxyl, lactones and phenols, these groups on carbon materials decompose upon heating by releasing CO and CO_2 at different temperatures, thus thermal desorption spectroscopy (TDS), also called TPD in a vacuum or in a helium stream, could be used for the study of surface oxides [37,

38]. The main functions of CA in catalysts lie in improvement of ruthenium distribution by influencing the amount of oxygen-containing functional groups and texture of AC [31, 32]. In this study, CA was used to create functional groups on activated carbon for the subsequent uniform dispersion of ruthenium nanoparticles. The profiles of He-TPD show that the amount of CO_2 and CO increase noticeably for the support treated with CA, indicating that the materials contain relatively more carboxyl and carbonyl groups whether at low temperature or at high temperature.

It has been widely accepted that each type of oxygen-containing functional groups decomposes to a defined product, e.g., a CO_2 peak results from carboxylic acids at low temperatures, or lactones at higher temperatures; carboxylic anhydrides originate both a CO and a CO_2 peak; phenols, ethers, and carbonyls (and quinones) originate a CO peak [37, 39–41]. The CO_2 peak (Fig. 2a) at low temperature (400–570 K) was attributed to carboxylic functional groups of CA [37, 42, 43]. CO_2 releases at higher temperatures might indicate the existence of different oxygen surface groups, such as carboxylic anhydrides and lactones. The carbonyl or lactone groups in the residual carbon gave a strong peak of CO in 1100 K (Fig. 2b). The peak site of CO for AC and CA4-AC is consistent, which illuminates the functional groups in the residual carbon are homologous. However, the amount of oxygen-containing groups on the surface of AC support is significantly little, which is not favorable for the high dispersion of Ru.

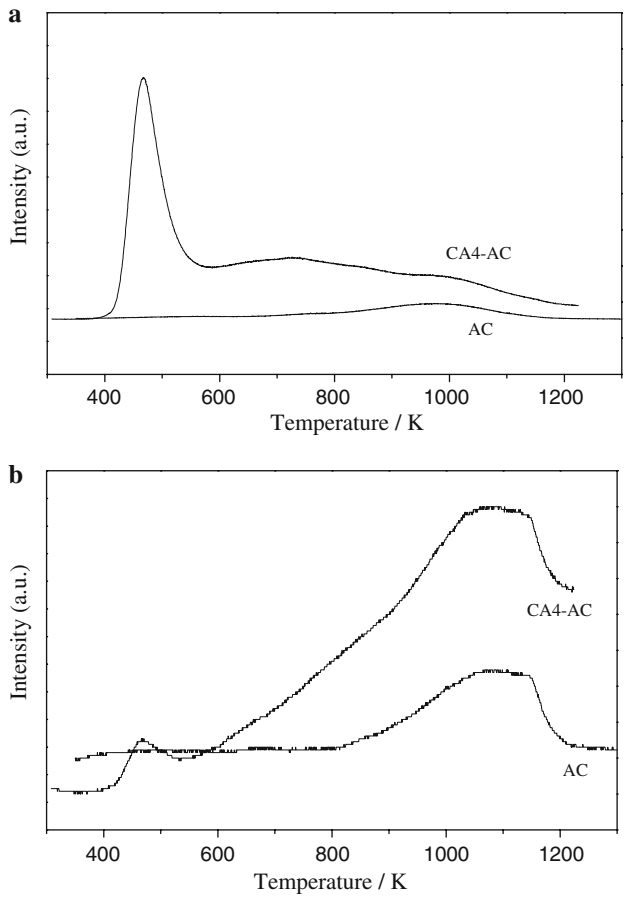

Fig. 2 TPD profiles of AC with different treatment (**a**) CO_2 (*m/e* = 44) and (**b**) CO (*m/e* = 28)

Citric acid functionalized AC contains more oxygen-containing groups on the AC. Plentiful oxygen-containing functional groups on the AC are very favorable to improve ruthenium dispersion and increase the B_5 active sites of Ru. Firstly, carboxyls and hydroxyls of CA provide nucleation sites for the deposition of highly dispersed $RuCl_3$ before thermal treatment. Then the anchorage is provided by carbonyls or lactones of CA residues capping the Ru and AC after reduction of catalysts. The residues of CA contain more oxygen-containing functional groups against the activated carbon from CO and CO_2 dates (Fig. 2), which is favorable for dispersion and anchorage of Ru. The anchorage of residues is favorable to decrease conglomerations of Ru at high reduction and reaction temperature.

3.3 Effect of Citric Acid on Size Distribution of Ru Particles

Figure 3 is TEM images of the Ru/AC catalyst. The Ru particles are high dispersed on the surface of AC, but the particle size is non-uniform. Some particles are ca. 1 nm in size, and the biggest particles are ca. 8 nm in size. A majority of particles vary from 3 to 5 nm in size [12]. TEM image of CA4 + Ru4/AC catalyst is shown in Fig. 4. The Ru particles are also high dispersed on the surface of AC. No apparent lumpy conglomerations of Ru can be found, which mean a high dispersion. Furthermore, most of the Ru particles are ca. 2–2.5 nm, which possessed more B_5-type active sites for the optimum crystal size [13]. The image revealed the presence of small and uniform Ru particles on the surface of catalyst treated with CA. TEM images of CA8 + Ru4/AC catalyst are shown in Fig. 5. The Ru particles are also high dispersed on the surface of AC. However, most of Ru particles are ca. 1.3–1.8 nm, which would significantly decrease the amount of B_5 active sites of CA8 + Ru4/AC catalyst as compared to the CA4 + Ru4/AC catalyst.

The TEM results show that CA influenced significantly on the size of Ru nanoparticles. The particles become uniform after adding CA, which could be explained as below. The surface of AC has many groups, such as carbonyls or lactones etc., whereas, the amount of functional groups on the AC is not plentiful. The deficiency of oxygen-containing functional groups leads to low distribution of $RuCl_3$ on the surface of AC, which brings a biggish particle size of Ru after reduction of Ru/AC catalyst.

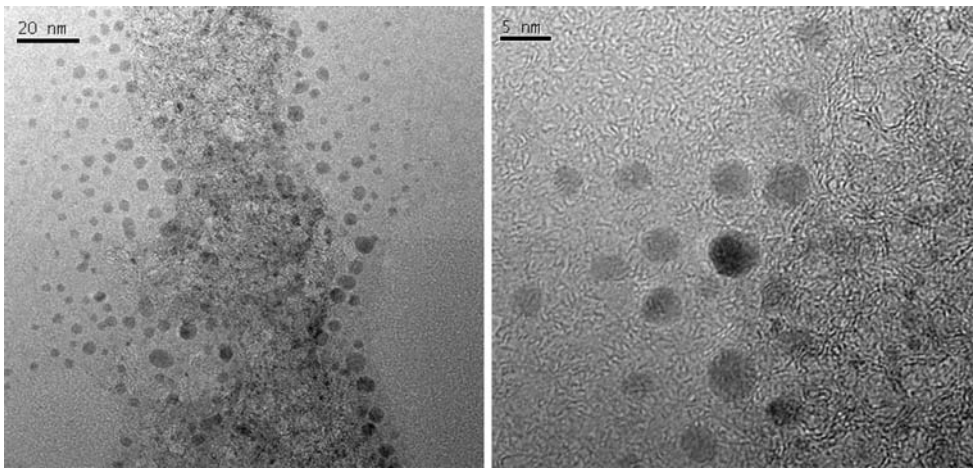

Fig. 3 TEM images of Ru/AC catalyst

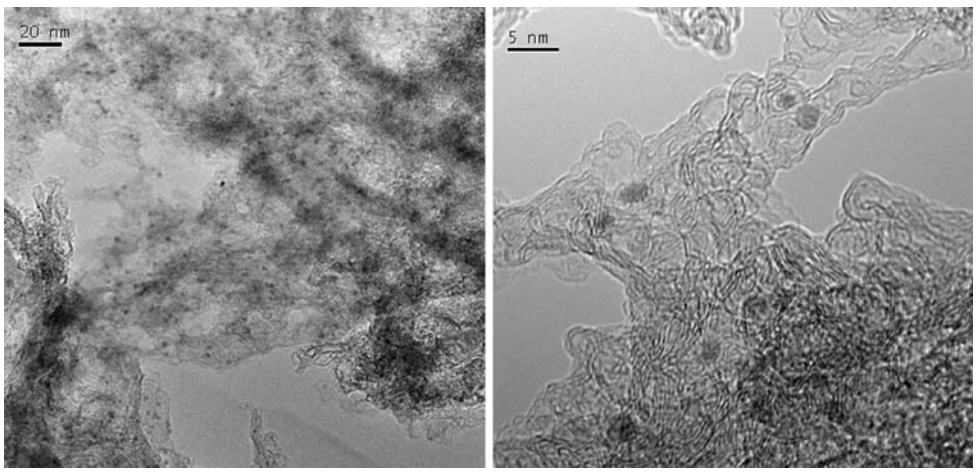

Fig. 4 TEM images of CA4 + Ru4/AC catalyst

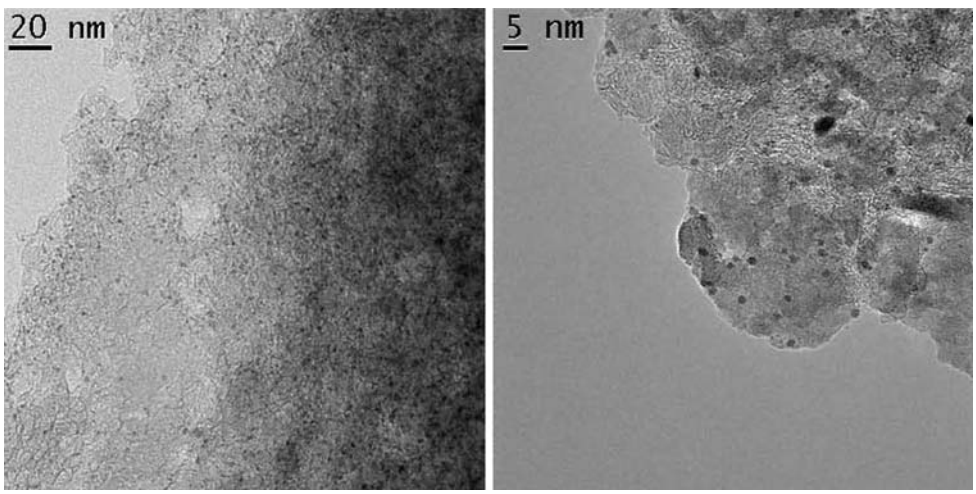

Fig. 5 TEM images of CA8 + Ru4/AC catalyst

Activated carbon materials can be easily functionalized using CA [32]. The functionalized groups on the surface of AC treated with CA are highly dispersed on the surface of support and there provide nucleation sites for the deposition of highly dispersed metal particles [32].

The B_5 sites are only present on crystals with a size larger than 1.5 nm. The maximum probability for B_5 sites is found for particles of 1.8–2.5 nm, and the probability monotonically decreases for particles larger than 2.5 nm in size [13]. In the Ru/AC catalyst some particle sizes are

between ca. 1 nm and ca. 8 nm, but most of particles are 3–5 nm in size. The wide range in size is disadvantageous to form more B_5-type sites. Addition of CA results in the size of Ru particles is 2–2.5 nm. The particle size distribution is under the optimal size range and Ru particles are well dispersed on the surface of AC, which suggested more B_5 sites exist in the CA4 + Ru4/AC catalyst. The uniformity in particle size could be a result of high dispersion of oxygen-containing functional groups on the AC surface.

The samples of the TEM test were treated with ultrasonic for 30 min. From Fig. 3 most of Ru particles were on carbon membrane for the Ru/AC catalyst, but most of Ru particles were on carbon support for the CA4 + Ru4/AC and CA8 + Ru4/AC catalysts (Figs. 4 and 5). The phenomena show that the Ru particles treated by CA were anchored on the surface of AC, otherwise, the phenomena from TEM images for the catalysts treated with CA should be consistent with the Ru/AC catalyst.

As can be seen from Table 3, the size of Ru particles determined from CO chemisorption is closely related to the content of CA. A suitable amount of CA is advantageous to improve the Ru dispersion, but the influence is not remarkable. Moreover, superfluous addition of CA decreases significantly the dispersion. CO chemisorption (Table 3) gives significantly higher values of the size of Ru compared to the TEM results for CA4 + Ru4/AC catalyst.

Comparing the CO chemisorption data collected from Table 3 and TEM results, it is clearly shown that the dispersion of ruthenium is closely related to the residues of CA. The Ru nanoparticles from TEM images are obviously less than from the CO chemisorption. Higher content of residues of CA results in higher coverage and lower dispersion of Ru. These illuminate the residues of CA has covered the partial surface of ruthenium. The partial coverage of Ru decreases the surface area of Ru. However, the actual size of Ru has not been influenced. Therefore, the partial coverage of Ru by the residues of CA lead to increase of particles size measured by CO chemisorption as compared to the TEM values. Although the Ru size could decrease further with the increase of CA in AC, but excessive addition of CA results in sharp decline of ruthenium size, which lead to much less B_5 active sites and worse activity for ammonia synthesis. In this paper, the optimal content of CA in the AC is 4 wt.%. From the results of TEM and CO chemisorption primary functions of CA are in two aspects, that is, dispersion of Ru by functional group of CA and isolation of Ru by the residues of CA.

3.4 TGA Analysis

To reveal further the effect of CA on the texture of AC and distribution of ruthenium, the TG of CA was measured in the nitrogen atmosphere. The sample for this measurement was prepared without the AC support. Figure 6 is the TGA profiles of CA. It can be seen that the CA began to decompose at 423 K and completely decomposed at 523 K. The residues are ca. 2 wt.% even if the decomposed temperature is over 850 K. The incomplete decomposition influences the texture of catalysts little (Table 2). However, the residual carbon has a great impact on the Ru dispersion (Table 3). The sharp decrease of dispersion further illuminated the partial residual carbon accumulated on the surface of ruthenium nanoparticles.

3.5 Effect of Citric Acid on Activity for Ammonia Synthesis

The dual promoter system (Ba and K) is introduced by the fellow causations. The unprompted Ru/AC catalysts are known to be almost inactive in ammonia synthesis, which is

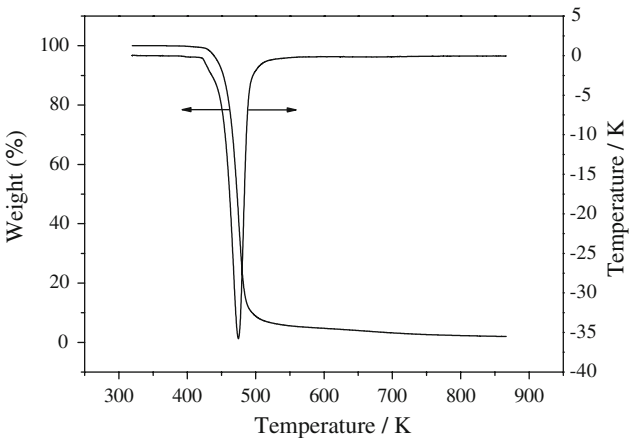

Fig. 6 TGA profiles of CA

Table 3 Effect of CA on Ru dispersion

Sample	S_{BET} (m^2/g)	CO uptake (μmol/g STP)	Ru dispersion (%)	Ru S_{BET} (m^2/g)	Ru size (nm)
AC	938	–	–	–	–
Ru/AC	847	126.03	33.15	121.10	4.0
CA2 + Ru4/AC	862	121.47	33.14	121.07	4.0
CA4 + Ru4/AC	863	130.31	35.58	129.97	3.7
CA8 + Ru4/AC	832	102.37	27.43	100.20	4.8
CA12 + Ru4/AC	855	80.45	21.16	77.30	6.3

Table 4 Effect of content of CA on the properties of catalysts

	Ammonia concentration[a] (vol.%)			TOF (10^{-2} S^{-1})			E_a (kJ/mol)
	673 K	698 K	723 K	673 K	698 K	723 K	
Ru4–Ba4–K12/AC	14.25	15.54	13.62	9.08	10.22	9.00	18.48
(CA2 + Ru4)–Ba4–K12/AC	14.94	16.21	14.76	9.68	10.71	9.54	15.80
(CA4 + Ru4)–Ba4–K12/AC	16.57	16.65	15.10	9.73	10.52	9.59	12.20
(CA8 + Ru4)–Ba4–K12/AC	14.63	15.95	14.01	9.27	10.10	8.88	13.40
(CA12 + Ru4)–Ba4–K12/AC	12.92	15.50	13.88	8.47	9.87	8.97	23.90

[a] Measured at 10 MPa and 10,000 h^{-1}

Experimental error of activity of ammonia synthesis is ca. 0.2 vol.%

not beneficial to investigate the performance of CA in catalysts. Ammonia synthesis reaction are known as an extremely structure sensitive activity on ruthenium. Ba is known as structural promoter [36, 44–46] or electronic promoter [47–50] in different literature. Generally, Ba and K promoters are known as structural promoter and electronic promoter, respectively [14, 36, 44]. The addition of CA improved the structure of Ru, and the addition of Ba in catalysts could exhibit the structure influence by the activity. The K promoter was introduced to significantly improve the activity of ammonia synthesis in lower temperature by eliminate the effect of chloride ion and acidic groups. The introduction of K is necessary to confirm the performance of CA without effect of electron withdrawing groups.

The effect of content of CA on the activity of ammonia synthesis is showed in Table 4. The impregnating solution is the mixed solution of CA and $RuCl_3$. Citric acid has a remarkable influence on the activity of catalysts for ammonia synthesis. The activity increase first and then decreases with the increase of content of CA in AC. The activity results show that the optimal amount of CA in support is 4 wt.%. In contrast to the Ru4–Ba4–K12/AC catalyst, the activity of the (CA4 + Ru4)–Ba4–K12/AC catalyst remarkably increases at the same reaction condition.

The value of activation energy and turnover frequency is shown in Table 4. The TOF and E_a results show that suitable addition of CA decrease the activation energy of the Ru4–Ba4–K12/AC catalyst and increase the turnover frequency. The low activation energy and high turnover frequency lead to high activity at 673 K for the (CA4 + Ru4)–Ba4–K12/AC. From the results of TEM and CO chemisorptions, the introduction of CA significantly improved the Ru size, therefore, the improved size of Ru between ca. 2 and 2.5 nm could remarkably increases the amount of B_5 active sites for the CA4 + Ru4/AC catalyst as compared to the Ru/AC catalyst. The significant increase of B_5 sites leads to the significant increase of turnover frequency and activity of ammonia synthesis. The present results show that there is no direct correlation between the activity of Ru and dispersion from CO chemisorption dates [12, 13, 51, 52]. However, the TEM results illuminate that the size distribution of Ru particles is directly correlated with the activities. The optimal size distribution of Ru particles between 1.8 and 2.5 nm would lead to higher activity of ammonia synthesis.

4 Conclusion

Citric acid is adsorbed preferentially to microporous surfaces of AC, which remarkably reduces specific surface area and pore volume of AC. Mass fraction of residues of CA in AC by thermal treatment has still ca. 2 wt.% even at 850 K. The residues have no significantly influence for the texture of the Ru/AC catalyst. The residues of CA contain more oxygen-containing functional groups against the AC, which is favorable for dispersion and anchorage of Ru.

TEM images show that the dispersion of Ru increases significantly and the nanoparticles sizes become more uniform with the addition of CA. CO chemisorption showed the dispersion of Ru treated with CA first increased after declining, which illuminated the surface of Ru was partially covered by the residues of CA.

Citric acid has a remarkable influence on turnover frequency, activation energy and activity of the catalysts for ammonia synthesis when the content of CA in AC is 4 wt.%. More works are under way to extend the CA method to decrease the unit amount of Ru in catalyst and increase the activity for ammonia synthesis.

Acknowledgments The present work was supported by the National Natural Science Foundation of China under Grant No. 20576021 and the National Science and Technology Support Program of China under Grant No. 2007BAE08B02

References

1. Miyazawa T, Koso S, Kunimori K, Tomishige K (2007) Appl Catal A: Gen 318:244
2. Miyazawa T, Kusunoki Y, Kunimori K, Tomishige K (2006) J Catal 240:213

3. Maris EP, Davis RJ (2007) J Catal 249:328
4. Bernas A, Kumar N, Laukkanen P, Väyrynen J, Salmi T, Murzin DY (2004) Appl Catal A: Gen 267:121
5. Nurunnabi M, Murata K, Okabe K, Inaba M, Takahara I (2007) Catal Commun 8:1531
6. Nurunnabi M, Murata K, Okabe K, Inaba M, Takahara I (2008) Appl Catal A: Gen 340:203
7. Shen X, Garces L-J, Ding Y, Laubernds K, Zerger RP, Aindow M, Neth EJ, Suib SL (2008) Appl Catal A: Gen 335:187
8. Zhong ZH, Aika K (1998) Inorg Chim Acta 280:183
9. Hinrichsen O, Rosowski F, Hornung A, Muhler M, Ertl G (1997) J Catal 165:33
10. Siporin SE, Davis RJ (2004) J Catal 225:359
11. Jacobsen CJH (2001) J Catal 200:1
12. Zeng HS, Inazu K, Aika K (2001) Appl Catal A: Gen 219:235
13. Jacobsen CJH, Dahl S, Hansen PL, Tornqvist E, Jensen L, Topsoe H, Prip DV, Moenshaug PB, Chorkendorff I (2000) J Mol Catal A: Chem 163:19
14. Guraya M, Sprenger S, Rarog-Pilecka W, Szmigiel D, Kowalczyk Z, Muhler M (2004) Appl Surf Sci 238:77
15. Rosowski F, Hornung A, Hinrichsen O, Herein D, Muhler M, Ertl G (1997) Appl Catal A: Gen 151:443
16. Zhong ZH, Aika K (1998) Inorg Chim Acta 280:183
17. Rossetti I, Forni L (2005) Appl Catal A: Gen 282:315
18. Lin B, Wang R, Lin J, Du S, Yu X, Wei K (2007) Catal Commun 8:1838
19. Han W, Liu H, Zhu H (2007) Catal Commun 8:351
20. Zawadzki M, Okal J (in press) Mater Res Bull
21. Jacobsen CJH, Dahl S, Hansen PL, Tornqvist E, Jensen L, Topsoe H, Prip DV, Moenshaug PB, Chorkendorff I (2000) J Mol Catal A: Chem 163:19
22. You ZX, Inazu K, Aika KI, Baba T (2007) J Catal 251:321
23. Han WF, Liu HZ, Zhu H (2007) Catal Commun 8:351
24. Xu QC, Lin JD, Fu XZ, Liao DW (2008) Catal Commun 9:1214
25. Wu S, Chen J, Zheng X, Zeng H, Zheng C, Guan N (2003) Chem Commun 2488
26. Kyotani T, Nakazaki S, Xu W-H, Tomita A (2001) Carbon 39:782
27. Hernadi K, Siska A, Thien-Nga L, Forr L, Kiricsi I (2001) Solid State Ionics 141–142:203
28. El-Hendawy, AA-N (2003) Carbon 41:713
29. El-Sheikh AH (2008) Talanta 75:127
30. Radkevich VZ, Senko TL, Wilson K, Grishenko LM, Zaderko AN, Diyuk VY (2008) Appl Catal A: Gen 335:241
31. Chen JP, Wu S, Chong K-H (2003) Carbon 41:1979
32. Poh CK, Lim SH, Pan H, Lin J, Lee JY (2008) J Power Sources 176:70
33. Jiang L, Gao L (2003) Carbon 41:2923
34. Rie N, Yoko N, Naoto O, Michio I (2006) New Carbon Mater 21:289
35. Liang CH, Wei ZB, Xin Q, Li C (2001) Appl Catal A: Gen 208:193
36. Kowalczyk Z, Jodzis S, Rarog W, Zielinski J, Pielaszek J, Presz A (1999) Appl Catal A: Gen 184:95
37. Boehm HP (2002) Carbon 40:145
38. Chen W, Pan X, Willinger MG, Su DS, Bao X (2006) J Am Chem Soc 128:3136
39. Figueiredo JL, Pereira MFR, Freitas MMA, Orfao JJM (1999) Carbon 37:1379
40. Liang Y, Zhang H, Yi B, Zhang Z, Tan Z (2005) Carbon 43:3144
41. Haydar S, Moreno-Castilla C, Ferro-Garcia MA, Carrasco-Marin F, Rivera-Utrilla J, Perrard A, Joly JP (2000) Carbon 38:1297
42. Nevskaia DM, Santianes A, Munoz V, Guerrero-Ruiz A (1999) Carbon 37:1065
43. Stavropoulos GG, Samaras P, Sakellaropoulos GP (2008) J Hazard Mater 151:414
44. Rarog W, Kowalczyk Z, Sentek J, Skladanowski D, Zielinski J (2000) Catal Lett 68:163
45. McClaine BC, Siporin SE, Davis RJ (2001) J Phys Chem B 105:7525
46. Szmigiel D, Bielawa H, Kurtz M, Hinrichsen O, Muhler M, Rarog W, Jodzis S, Kowalczyk Z, Znak L, Zielinski J (2002) J Catal 205:205
47. Hansen TW, Hansen PL, Dahl S, Jacobsen CJH (2002) Catal Lett 84:7
48. Siporin SE, Davis RJ, Rarog-Pilecka W, Szmigiel D, Kowalczyk Z (2004) Catal Lett 93:61
49. Hansen TW, Wagner JB, Hansen PL, Dahl S, Topsoe H, Jacobsen CJH (2001) Science 294:1508
50. Rossetti I, Pernicone N, Forni L (2001) Appl Catal A: Gen 208:271
51. Kowalczyk Z, Krukowski M, Rarog-Pilecka W, Szmigiel D, Zielinski J (2003) Appl Catal A: Gen 248:67
52. Szmigiel D, Rarog-Pilecka W, Miskiewicz E, Glinski M, Kielak M, Kaszkur M, Kowalczyk Z (2004) Appl Catal A: Gen 273:105